Technology of the Science and Technology Agency of the Japanese Government.

**Registry No.** PTFE, 9002-84-0; PVDF, 24937-79-9.

## References and Notes


(1) Hofmann, S.; Sanz, J. M. *Fresenins' Z. Anal. Chem.* **1983**, *314*, 215.
(2) Mathieu, H. J.; Landolt, D. *Appl. Surf. Sci.* **1982**, *10*, 100.
(3) Kelly, R. *Nucl. Instr. Methods* **1978**, *149*, 553.
(4) Holm, R.; Storp, S. *Appl. Phys.* **1976**, *9*, 217.
(5) Storp, S.; Holm, R. *J. Electron Spectrosc. Relat. Phenom.* **1979**, *16*, 183.
(6) Katrib, A. *J. Electron Spectrosc. Relat. Phenom.* **1980**, *18*, 275.
(7) Kim, K. S.; Winograd, N. *Surf. Sci.* **1974**, *43*, 625.
(8) Hufner, S.; Cohen, R. L.; Wertheim, G. K. *Physica Scr.* **1972**, *5*, 91.
(9) Tsanz, T.; Coyle, G. J.; Adler, I.; Yin, L. *J. Electron Spectrosc. Relat. Phenom.* **1979**, *16*, 389.
(10) Shimizu, H.; Ono, M.; Nakayama, K. *Surf. Sci.* **1973**, *36*, 817.
(11) Toth, A.; Bertoti, I.; Szekely, T.; Mohai, M. *Surf. Interface Anal.* **1985**, *7*, 282.
(12) Ulleving, D. M.; Evans, J. F. *Anal. Chem.* **1980**, *52*, 1467.
(13) Briggs, D.; Wootton, A. B. *Surf. Interface Anal.* **1982**, *4*, 109.
(14) Gardella, J. A., Jr.; Hercules, D. M. *Anal. Chem.* **1980**, *52*, 226.
(15) Gardella, J. A., Jr.; Hercules, D. M. *Anal. Chem.* **1981**, *53*, 1879.
(16) Briggs, D. *Surf. Interface Anal.* **1982**, *4*, 151.
(17) Briggs, D. *Surf. Interface Anal.* **1983**, *5*, 113.
(18) Clark, D. T.; Feast, W. J.; Kilcast, D.; Musgrave, W. K. R. *J. Polym. Sci., Polym. Chem. Ed.* **1973**, *11*, 389.
(19) Dwight, D. W.; Riggs, W. M. *J. Colloid Interface Sci.* **1974**, *47*, 650.
(20) Delhalle, J.; Delhalle, S.; Andre, J. M.; Pireaux, J. J.; Riga, J.; Caudano, R.; Verbist, J. J. *J. Electron Spectrosc. Relat. Phenom.* **1977**, *12*, 293.
(21) Clark, D. T.; Feast, W. J.; Tweedale, P. J.; Thomas, H. R. *J. Polym. Sci., Polym. Chem. Ed.* **1980**, *18*, 1651.
(22) Nagarajan, S.; Stachurski, Z. H.; Hughes, M. E.; Larkins, F. P. *J. Polym. Sci., Polym. Phys. Ed.* **1982**, *20*, 1001.
(23) Takahagi, T.; Nakayama, Y.; Soeda, F.; Ishitani, A., to be published.
(24) Siegbahn, K.; Nordling, C.; Johansson, G.; Hedman, J.; Heden, P. F.; Hamrin, K.; Gelius, U.; Bergmark, T.; Werme, L. O.; Manne, R.; Baer, Y. *ESCA Applied to Free Molecules*; North-Holland Publishing Co.: Amsterdam, 1969; pp 113-120.
(25) Clark, D. T.; Thomas, H. R. *J. Polym. Sci., Polym. Chem. Ed.* **1977**, *15*, 2843.
(26) Fadley, C. S. In *Electron Spectroscopy: Theory, Techniques and Applications*; Brundle, C. R., Baker, A. D., Eds.; Academic: New York, 1978; pp 124-131.
(27) Gardella, J. A., Jr.; Chin, R. L.; Ferguson, S. A.; Farrow, M. M. *J. Electron Spectrosc. Relat. Phenom.* **1984**, *34*, 97.


# Time-of-Flight Secondary Ion Mass Spectrometry of Polymers in the Mass Range 500–10 000

**Ioannis V. Bletsos and David M. Hercules***

*Department of Chemistry, University of Pittsburgh, Pittsburgh, Pennsylvania 15260*

**Dieter vanLeyen and Alfred Benninghoven**

*Physikalisches Institut der Universität Münster, D-4400 Münster, Federal Republic of Germany.* *Received May 22, 1986*

ABSTRACT: Secondary ion mass spectra of a poly(dimethylsiloxane), a polyurethane, and polystyrenes are presented. The spectra were obtained by a time-of-flight secondary ion mass spectrometer equipped with a mass-selected primary ion source, an angle- and time-focusing time-of-flight analyzer, and a single-ion-counting detector. Fragmentation in the low-mass range ($m/z \leq 500$) provided structural information about the repeat unit. $Ag^+$ and $Na^+$ cationization of polymer fragments and intact polymer molecules containing large numbers of repeat units in the high-mass range ($m/z$ 500–10 000) allowed identification of the polymers studied. Fragmentation patterns were unique for polymers having different repeat units but of equal mass; distinguishing between such polymers was possible. Oligomer distributions for polystyrene standards obtained from the mass spectrum compared well with distributions determined by other techniques (e.g., gel permeation chromatography).

## Introduction

Polymers typically exhibit low volatility and, therefore, pose serious problems for ion formation in mass spectrometry (MS). To date, volatilization methods coupled to MS for characterization of polymers primarily involved pyrolysis (PY-MS). Pyrolysis degrades polymers such that characteristic fragment ions can be used for polymer identification.[1] PY-MS has been used to characterize polymers, polymer blends, and additives;[2] when PY-MS was coupled to gas chromatography, the composition[3] and head-to-head or head-to-tail additions[4,5] for styrene/methacrylate copolymers could be determined. Copolymers have been differentiated from homopolymer mixtures with PY-MS by detection of dimer and trimer fragments.[6] Polyurethanes have been studied by PY-MS; some information about the nature of polyols and isocyanates could be deduced.[7]

A major concern in the PY-MS experiment is reproducibility because decomposition processes are time and temperature dependent. If the pyrolysis temperature is too low, incomplete decomposition occurs. Secondary reactions during pyrolysis are also troublesome because they alter the primary fragments and complicate interpretation of the mass spectrum. If the pyrolysis temperature is too high, noncharacteristic low $m/z$ fragments dominate the mass spectrum. Even at the optimum temperature, the highly energetic pyrolytic processes produce low $m/z$ fragments. These fragments are usually common to a class of polymers, and therefore identification of polymers with similar repeat units often becomes difficult.

The invention of softer volatilization and ionization sources, combined with instrumental advances, has expanded MS to a higher mass range so that sequences of repeat units and oligomer distributions can be observed.[9,10] Field desorption mass spectrometry (FDMS) has been applied extensively to the analysis of polymers.[8,9] Quasi-molecular ions from FDMS exhibit high intensity compared to that of low $m/z$ fragments; FDMS can be used for the determination of oligomer distributions. Accurate molecular weight averages of low molecular weight poly-

0024-9297/87/2220-0407$01.50/0 

mers have been obtained from relative intensities of quasi-molecular ions with appropriate corrections for isotopic abundances.[10-12] Desorption of quasi-molecular ions depends on emitter heating current, and fragmentation is a function of the field strength applied; therefore, many spectra must be averaged to give accurate molecular weight distributions. Accurate molecular weight distributions have been determined by FDMS mainly for polar polymers (e.g., poly(ethylene glycols), etc.). Other polymers (e.g., alkylated phenol/formaldehyde resins) termed "poor desorbers" gave consistently low molecular weight values.[13] Limited control of the ionization processes and elaborate sample preparation affect the precision of the technique.

Electrohydrodynamic MS (EHDMS) has been applied successfully to the analysis of poly(ethylene glycols); reliable molecular weight distributions were determined by spectral averaging.[14] However, EHDMS is limited to polymers that contain polar groups, so they can be dissolved in glycerol and can readily form quasi-molecular ions via cation attachment or proton abstraction.

Analysis of polyethers by $^{252}Cf$ plasma desorption mass spectrometry ($^{252}Cf$-PDMS) produced series of oligomeric quasi-molecular ions.[15] Although processes producing low-mass fragments were prominent over the long data-acquisition time required, intensity distributions of quasi-molecular ions were indicative of the average molecular weights of polyethers.

Spectra of polymers obtained by laser mass spectrometry (LMS)[16-18] are characteristic both of the backbone of straight chain polymers and of pendant functional groups. In general, only small fragments or cationized clusters containing up to one or two repeat units have been observed by LMS. This could be due either to degradation by the highly energetic laser or to insufficient sensitivity of the detector used. A quantitative study of poly(fluoroethylene) by LMS allowed the determination of the percent of head-to-tail, head-to-head, and tail-to-tail additions. The results compared well with those obtained by $^{19}F$ NMR spectroscopy.[19] Accurate molecular weight averages have been obtained by LMS for some low molecular weight polyglycols using peak intensities of cationized polymer chains.[20] Laser desorption coupled to Fourier transform mass spectrometry (LD-FTMS) seems to be promising for polymer analysis because it combines detection capabilities at high-mass range with good resolution. Mass spectra indicative of molecular weight distributions have been obtained by LD-FTMS for a variety of polymers.[21,22] Calculated molecular weights agree well with those determined by other techniques (e.g., end point titration).[22]

Static secondary ion mass spectrometry (SIMS)[23] has been applied to structural characterization[24-27] and surface analysis of polymers.[28,29] Polymers can be identified from fingerprint spectra or from fragments characteristic of the backbone and pendant groups. SIMS reports have not yet appeared on direct analysis of low molecular weight oligomers. Liquid matrix SIMS (FABMS) has provided only approximate oligomer distributions; intensities attributed to low mass oligomers tend to be too high due to contributions from extensive fragmentation of higher mass oligomers.[30]

SIMS spectra of polymers have been confined to the low-mass range ($m/z \leq 500$) mainly due to the mass analyzers used (e.g., quadrupole). With the advent of high-transmission time-of-flight mass analyzers coupled to sensitive detection systems (e.g., postacceleration and single ion counting), primary ion dosages have been reduced considerably, minimizing fragmentation; detection of high mass ions (up to $m/z \sim 5000$) has been dramatically increased.[31] A series of aliphatic polyamides (nylons) was studied by time-of-flight secondary ion mass spectrometry (TOF-SIMS).[34] Cationization of the repeat unit with $Ag^+$ and $Na^+$ produced high-mass ions characteristic of the type of nylon and the repeat unit sequence in the polymer chain. Polymer fragments cationized with $Ag^+$ and $Na^+$, containing as many as 24 repeat units (nylon 6) and as high as $m/z \sim 3500$ [nylon 66($\alpha$6)], were detected.

In this report we present secondary ion mass spectra of diverse polymers: a poly(dimethylsiloxane), a polyurethane, and polystyrenes. The spectra were obtained by a time-of-flight secondary ion mass spectrometer, equipped with a mass-selected pulsed primary ion source, an angle- and time-focusing time-of-flight analyzer, and a single-ion-counting detector.[32,33] Fragmentation in the low-mass range provided some structural information about the repeat unit. $Ag^+$ and $Na^+$ cationization of polymer fragments containing large numbers of repeat units at high $m/z$ allowed identification of the polymer. Fragmentation patterns were unique for polymers having different repeat units but of equal mass; distinguishing between such polymers was possible. Oligomer distributions obtained from mass spectra compared well with distributions determined by other techniques (e.g., gel permeation chromatography) for the same polymers. The purpose of the present paper is to present an overview of the capabilities of TOF-SIMS for polymer characterization. Each of the topics to be addressed here will be published in greater detail elsewhere.

## Experimental Section

**Sample Preparation.** Polystyrene (Scientific Polymer Products, Ontario, NY), polystyrene molecular weight standard (Polymer Laboratories Inc., Amherst, MA), and poly(dimethylsiloxane) (Polysciences, Warrington, PA) samples were dissolved in toluene. The polyurethane (Mobay Chemical Inc., Pittsburgh, PA) was dissolved in dimethylformamide (DMF). The concentrations of the solutions were in the range $1 \times 10^{-2}$–$1 \times 10^{-3}$ M with respect to the repeat unit. A 1–5-$\mu$L quantity of each solution was deposited on 100 mm$^2$ of a silver substrate which had been cleaned by etching in nitric acid (20 vol %). Approximately 1–5 $\mu$g of each polymer was deposited on the silver substrate for analysis.

**Instrumentation.** The time-of-flight mass spectrometer used was specially designed for SIMS applications.[32,33] It has high transmission and detects ions in the mass range $m/z$ 0–10 000 simultaneously. A schematic of the apparatus is shown in Figure 1.[32,33] A continuous beam of primary argon ions (1) is produced in a conventional electron impact source. Acceleration to 8 keV and focusing are accomplished by slit electrodes. By application of a 5-kV pulse for 1 $\mu$s to a parallel plate deflection system (2), a short bunch of ions is chopped from the continuous beam and deflected into a magnetic sector field (3) where it is mass separated. The path lengths of the ions in the packet are matched so that time focusing is achieved. This system produces packets of 100–10 000 primary ions focused on a spot of about 1 mm$^2$ on the target (6). The pulse repetition rate can be adjusted up to 40 kHz, the pulse duration is $\leq$10 ns, and the energy of the ions is approximately 12 keV.

Secondary ions are extracted from the sample and accelerated by an ion lens operating at 3 kV into a time-of-flight mass analyzer (7) of the Poschenrieder type.[33] The mass of the secondary ions is determined by measurement of the time-of-flight through a combination of an electrostatic sector field (8) with two linear drift spaces (7, 9). This arrangement provides first-order focusing of energy and angle, thus improving the mass resolution, which is limited initially by the energy spread of the secondary ions.

To enhance detection efficiency, especially for high masses, a postacceleration voltage of up to 20 kV is applied to the entrance of the detector unit (10). The detector consists of a channel plate for ion–electron conversion (11) and optical signal coupling to a scintillator (12) and photomultiplier (13). Single-ion counting

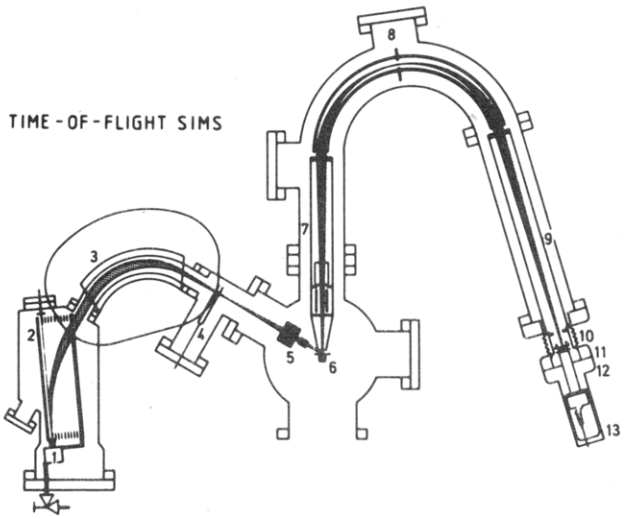


**Figure 1.** Schematic of TOF-SIMS:[31,32] (1) primary ion source; (2) deflector; (3) bunching magnet; (4) start pulse multiplier; (5) ion lens; (6) sample target; (7, 9) linear drift paths; (8) 163° toroidal condenser; (10) postacceleration gap; (11) channel plate; (12) scintillator; (13) photomultiplier.

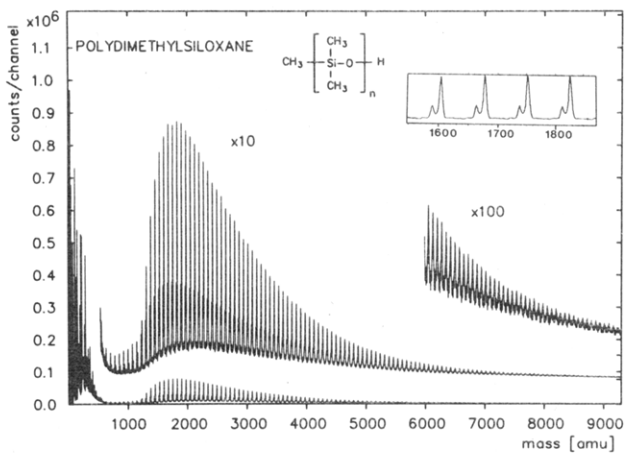


**Figure 2.** TOF-SIMS spectrum of poly(dimethylsiloxane) in the range $m/z$ 0–9300. The most intense peaks are due to desorption of intact polymer molecules cationized with $Ag^+$ $(nR + CH_3 + H + Ag)^+$. The peaks appearing in the inset on the low $m/z$ side of the most intense peaks are due to fragments of poly(dimethylsiloxane) cationized with $Ag^+$ and containing a large number of repeat units $(nR + Ag)^+$. The oligomer distribution of this polymer is not known.

is used to enhance the signal-to-background ratio and to reduce mass discrimination of ions having the same $m/z$. During the measurement a target area of about 1 $mm^2$ is bombarded by 12-keV $Ar^+$ ions with an average current of 30 pA for 60–300 s, corresponding to a primary ion current density of $10^{-9}$ $A/cm^2$ (static SIMS).

## Results and Discussion

**Poly(dimethylsiloxane).** A time-of-flight SIMS (TOF-SIMS) spectrum of poly(dimethylsiloxane) (PDMSO) is shown in Figure 2. The distribution of peak intensities observed in the range $m/z$ 500–9300 reflects the oligomer distribution of PDMSO. The spacing between consecutive peaks is equal to the repeat unit (R) of PDMSO (R = 74 amu) from which the polymer can be identified. The peaks observed in the spectrum are due to polymer fragments and polymer molecules cationized with $Ag^+$. In SIMS the impact of primary ions desorbs molecules and fragments and generates $Ag^+$ ions by sputtering the substrate.[35] Cationization of molecules and fragments can be accounted for by this mechanism.

**Table I**
**Ions Observed for PDMSO in the Range $m/z$ 800–2500**

| $n$ | $(nR + CH_3 + H + Ag)^+$ | $(nR + Ag)^+$ |
|---|---|---|
| 10 | 863 (2601)[a] | 847 (5853), 849 (6243)[b] |
| 11 | 937 (2862) | 921 (7154) |
| 12 | 1011 (3428) | 995 (7382) |
| 13 | 1085 (3559) | 1069 (8831) |
| 14 | 1159 (5800) | 1143 (9227) |
| 15 | 1233 (15093) | 1217 (10875) |
| 16 | 1307 (30714) | 1291 (13595) |
| 17 | 1381 (45567) | 1365 (17371) |
| 18 | 1455 (55889) | 1439 (19133) |
| 19 | 1529 (62434) | 1513 (20140) |
| 20 | 1603 (67302) | 1587 (20761) |
| 21 | 1677 (69013) | 1661 (20875) |
| 22 | 1751 (68634) | 1735 (20990) |
| 23 | 1825 (69355) | 1809 (19961) |
| 24 | 1899 (68923) | 1883 (19046) |
| 25 | 1973 (65182) | 1957 (17571) |
| 26 | 2047 (63936) | 2031 (16324) |
| 27 | 2121 (63028) | 2105 (15983) |
| 28 | 2195 (59288) | 2179 (15505) |
| 29 | 2269 (56907) | 2253 (15432) |
| 30 | 2343 (54013) | 2327 (14950) |
| 31 | 2417 (49190) | 2401 (13599) |
| 32 | 2491 (49262) | 2475 (12538) |

[a] Peaks due to silver isotopes not resolved. [b] $m/z$ of ions; intensity in parentheses (counts/channel).

Generally cationization stabilizes molecular and fragment ions.[36] Cationization with silver is commonly observed in SIMS experiments when Ag foils are used as substrates. Silver ions sputtered from the substrate are usually the most abundant cations observed in the mass spectrum.

In the mass range $m/z$ 500–9600 the TOF-SIMS spectrum of PDMSO results from a convolution of two processes occurring during the SIMS experiment. First, desorption of intact polymer chains generates the most intense series of peaks in the high-mass range of the spectrum ($m/z$ 500–9600). Desorption of intact polymer chains yields a series of peaks corresponding to $(nR + CH_3 + H + Ag)^+$, where $n$ = 8, 9, 10, ..., 128. The ions detected in this series have mass values corresponding to the presence of a terminal methyl group, indicating that desorption of polymer molecules occurs without fragmentation. The intensity distribution of the peaks of this series reflects the oligomer distribution of the PDMSO studied. Second, fragmentation of polymer chains is evident from peaks on the low-mass side of the main peaks, as shown in the inset of Figure 2; the same fragment ion peaks appear as the shaded region of lower intensity in the spectrum of Figure 2 due to the extended mass scale used in the spectrum. This second series of peaks corresponds to $(nR + Ag)^+$, where $n$ = 7, 8, 9, ..., 70. These peaks result from fragments produced by cleavage of the –Si–O– bond along the polymer backbone.

Further fragmentation within a repeat unit is not observed; i.e., no fragment ions of the type $(nR - O + Ag)^+$, $(nR - mCH_3 + Ag)^+$, or $[nR - Si(CH_3)_2 + Ag]^+$ are detected. The spacing between consecutive peaks in both the desorption, $(nR + CH_3 + H + Ag)^+$, and fragmentation, $(nR + Ag)^+$, series corresponds to the mass of the polymer repeat unit (R = 74 amu). Peaks for both series are tabulated for the range $m/z$ 800–2500 in Table I. The intensity maximum of the $(nR + CH_3 + H + Ag)^+$ series occurs at $m/z$ 1825, $n$ = 23; after $n$ = 23, the intensity decreases approximately exponentially as a function of $m/z$. The intensity maximum of the $(nR + Ag)^+$ series occurs at $m/z$ 1735, $n$ = 22. Up to $m/z$ 1143, $n$ = 14, the $(nR + Ag)^+$ series is more intense than $(nR + CH_3 + H + Ag)^+$. A transition in intensity occurs at $n$ = 15; from

**Table II**
**Ions Observed for PDMSO below $m/z$ 500**

| Significant Peaks | | |
|---|---|---|
| ion | $n$ | $m/z$ |
| $CH_2Si(CH_3)O[Si(CH_3)_2O]_n^+$ | 0 | 73 |
| | 1 | 147 |
| | 2 | 221 |
| | 3 | 295 |
| | 4 | 369 |
| | 5 | 443 |
| $SiO[Si(CH_3)_2O]_n^+$ | 1 | 118 |
| | 2 | 192 |
| | 3 | 266 |
| $[Si(CH_3)_2O]_nSi(CH_3)_2OH^+$ | 0 | 75 |
| | 1 | 149 |
| | 2 | 223 |
| | 3 | 297 |
| $Si(CH_3)[OSi(CH_3)_2]_n^+$ | 0 | 43 |
| | 1 | 117 |
| | 2 | 191 |
| | 3 | 265 |
| | 4 | 339 |
| | 5 | 413 |
| | 6 | 487 |
| $CH_2Si(CH_3)[OSi(CH_3)_2]_n^+$ | 0 | 57 |
| | 1 | 131 |
| | 2 | 205 |
| | 3 | 279 |
| | 4 | 353 |
| | 5 | 427 |
| | 6 | 501 |
| $Si(CH_3)O[Si(CH_3)_2O]_n^+$ | 0 | 59 |
| | 1 | 133 |
| | 2 | 207 |
| | 3 | 281 |
| | 4 | 355 |
| | 5 | 429 |
| | 6 | 503 |
| $[Si(CH_3)_2O]_n^+$ | 1 | 74 |
| | 2 | 148 |
| | 3 | 222 |
| $(CH_3)_{n-3}[Si(CH_3)O]_nO^+$ | 3 | 193 |
| | 4 | 267 |
| | 5 | 341 |
| | 6 | 415 |

| Other Peaks | |
|---|---|
| ion | $m/z$ |
| $Si^+$ | 28, 29, 30 |
| $SiOH^+$ | 45 |
| $Si(CH_3)_2^+$ | 58 |
| $Si(CH_3)O^+$ | 89 |
| $CH_3(SiO_2)^+$ | 103 |
| $(CH_3SiO)_3^+$ | 177 |
| $CH_3[Si(CH_3)O]_4^+$ | 251 |
| $(CH_3)_2[Si(CH_3)O]_5^+$ | 325 |
| $(CH_3)_3[Si(CH_3)O]_6^+$ | 399 |
| $[Si(CH_3)_2O]_5Si(CH_3)OSiO^+$ | 473 |

that point on the $(nR + CH_3 + H + Ag)^+$ becomes the more intense series of peaks. Noise levels are about 350 counts/channel around $m/z$ 1700, and the mass spectrum shows a signal-to-noise ratio of approximately 200.

Extensive fragmentation of PDMSO is evident below $m/z$ 500. Structurally significant fragments containing C, H, Si, and O are detected in great abundance (ca. (1–9) $\times 10^5$ counts/channel) in the low $m/z$ range of the spectrum ($m/z$ <500). The peaks and their corresponding structures are shown in Table II. Peaks result from ions produced by fragmentation processes corresponding to loss of hydrogen, methyl, hydroxyl, or methoxy groups from polymer fragments containing an integral number of repeat units.

Loss of a proton from PDMSO fragments containing an integral number of repeat units gives rise to ions corresponding to $(nR - H)^+$, $n$ = 1, 2, 3, ..., 6, as shown in Table II. Fragments containing an integral number of repeat unit and a terminal $Si(CH_3)_3$ group, $[nR + Si(CH_3)_3]^+$, $n$ = 0, 1, 2, ..., 5, give rise to ions having the same $m/z$ as the $(nR - H)^+$ series. Ions resulting from the loss of one methyl group constitute the $(nR - CH_3)^+$ series, $n$ = 1, 2, 3, ..., 7. Loss of two methyl groups from fragments consisting of an integral number of repeat units corresponds to the $(nR - 2CH_3)^+$ series, $n$ = 2, 3, 4. Ions resulting from the loss of one hydroxyl group correspond to the $(nR - OH)^+$ series, $n$ = 1, 2, 3, ..., 7. Loss of one methoxy group produces a series of ions having the formula $(nR - CH_3O)^+$, $n$ = 1, 2, 3, ..., 7. Addition of a proton is observed for ions up to the tetramer $(nR + H)^+$, $n$ = 1, 2, 3, 4 ($m/z$ 75, 149, 223, 297). The ions at $m/z$ 74, 148, and 222 are the monomer and cyclic dimethylsiloxanes, $nR^+$, $n$ = 2, 3. This series of cyclic dimethylsiloxanes might have been produced during the synthesis of PDMSO by termination of the linear chain growth by cyclization at early chain growth stages.[37] The ions at $m/z$ 193, 267, 341, and 415 probably are cyclic species with a bridging oxygen atom formed by decomposition of cyclic dimethylsiloxanes.[38]

Two major processes that a polymer undergoes during the SIMS experiment are seen in the PDMSO spectrum. Desorption of whole polymer molecules generates the oligomer distribution for the polymer. Fragmentation produces large chain fragments composed of many repeat units. Extensive degradation of the polymer, which produces structurally significant fragments, is evident at $m/z$ ≤500. The highest mass ion detected was at approximately $m/z$ 9600 and is cationized with a single silver ion; it has a terminal methyl group and consists of 128 repeat units of PDMSO. It is possible that ions of even higher mass ($m/z \geq 10^4$) were produced. The mass registration of the spectrum, however, ended at $m/z$ 9600 due to settings of the extraction voltage (5 kV) and the postacceleration (15 kV).

**Polyurethanes.** Polyurethanes (PUR) present a special challenge for characterization by MS. Pyrolysis coupled to mass spectrometry has been used to characterize PUR, but the degradative nature of the technique has restricted the study of PUR to the low-mass range ($m/z$ ≤500).[7] TOF-SIMS studies of nylons[34] indicated that the technique might be used successfully to characterize PUR. The primary objective in the characterization of PUR is identification of the $R_1$, $R_2$, and $R_3$ groups in the general PUR formula H–[[$OR_1$]$_m$$OR_2OC(=O)NHR_3NHC(=O)$]$_n$–[$OR_1$]$_m$–$OR_2OH$, where $R_1$ = –[$CH_2$]$_k$–$OC(=O)$–[$CH_2$]$_l$–$C(=O)$, $R_2$ = –[$CH_2$]$_k$–, and $R_3$ = 1,4-$C_6H_4$–$CH_2$–1,4-$C_6H_4$, –[$CH_2$]$_6$–, 1,4-$C_6H_{10}$–$CH_2$–1,4-$C_6H_{10}$, or 1,3-$C_6H_3CH_3$. We present here a report of our studies of PUR using TOF-SIMS. We believe this to be the first report in which high-mass fragments of PUR were observed by mass spectrometry. Detailed characterization of a variety of PUR samples using TOF-SIMS will be published elsewhere.[39]

In general, fragments characteristic of the PUR backbone, the $R_1$, $R_2$, and $R_3$ groups, carbon clusters, and $Ag^+$ clusters dominate the PUR TOF-SIMS spectra in the low-mass range ($m/z$ <400). This information is useful and is as much as PY-MS could optimally provide.

A section of the TOF-SIMS spectrum of a PUR (I) in the range $m/z$ 650–1650 is shown in Figure 3. The formula of the PUR used in this example is given in I. Bond cleavage produces four different kinds of fragments (labeled A through D) cationized with $Ag^+$ or $Na^+$ and observed in the range $m/z$ 400–3000. The highest $m/z$ peak in the spectrum was observed at $m/z$ 3052 and corresponds

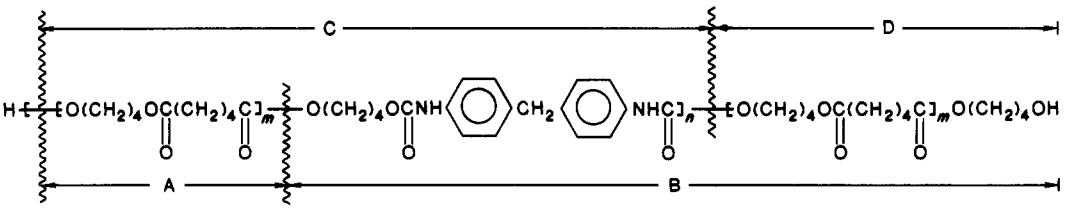

I

to a PUR fragment cationized with $Na^+$; the presence of $Na^+$ is due to contamination from the solvent (DMF). Fragmentation patterns are consistent throughout the detectable mass range and correspond to four well-defined series of peaks: $(A + M)^+$, $(B + M)^+$, $(C + M)^+$, and $(D + M)^+$, where M = Ag, Na. The peaks in the spectrum of Figure 3 are identified by the letter of the series to which they correspond. All peaks for the PUR studied are given in Table III for the range $m/z$ 600–1700. From the position of a peak and the spacing between consecutive peaks of the same series, the structures of the PUR repeat unit and terminal groups can be determined. For example, the peaks at $m/z$ 707, 709 correspond to $-[[O(CH_2)_4OC(=O)(CH_2)_4C(=O)]_3- + Ag]^+$, and the peak at $m/z$ 852 corresponds to $-[O(CH_2)_4OC(=O)NH-1,4-C_6H_4-CH_2-1,4-C_6H_4-NHC(=O)-[O(CH_2)_4OC(=O)(CH_2)_4C(=O)]_2-O(CH_2)_4OH + Na]^+$.

The fragmentation pattern observed in the TOF-SIMS spectrum of the PUR example presented here is characteristic of all PUR samples studied. Therefore, the major fragments of the PUR under $Ar^+$ bombardment can be generalized as follows: fragment A, $-[[OR_1]_x + M]^+$; fragment B, $(H)-[OR_2OC(=O)NHR_3NHC(=O)-[OR_1]_x-OR_2OH + M]^+$; fragment C, $-[[OR_1]_x-OR_2OC(=O)-NHR_3NHC(=O)- + M]^+$; fragment D, $-[[OR_2]_x-OR_3OH + M]^+$. Peaks corresponding to the B series are reported here as cationized polymer fragments, but they could also be due to desorption of cationized PUR oligomers. The difference between the two possible structures is one hydrogen; the resolution of the present instrument ($m/\Delta m \sim 1000$) is not sufficient to distinguish between the two possible structures.

The difference in mass between an A fragment, i.e., $-[(OR_1)_x- + M]^+$, and a C fragment, i.e., $-[[OR_1]_x-OR_2OC(=O)NHR_3NHC(=O)- + M]^+$, corresponds to the mass of $-[OR_2OC(=O)NHR_3NHC(=O)]$. Specifically for the PUR of Figure 3, the difference between the peaks at $m/z$ 1163 due to $-[(O(CH_2)_4OC(=O)(CH_2)_4C(=O))_4O-(CH_2)_4OC(=O)NH-1,4-C_6H_4-CH_2-1,4-C_6H_4-NHC(=O) + Na]^+$ and $m/z$ 823 due to $-[(O(CH_2)_4OC(=O)(CH_2)_4C(=O))_4 + Na]^+$ is $m/z$ 340, which is the mass of $-[O-(CH_2)_4OC(=O)NH-1,4-C_6H_4-CH_2-1,4-C_6H_4-NHC(=O)]-$. From such well-defined fragmentation patterns the structures of the diols, esters, and isocyanates used in the synthesis of PUR can be identified, and their sequence in the repeat unit and terminal groups can be determined. Low molecular weight PUR oligomers ($M_n < 10000$) might be detected intact, and the number of diol or ester groups per repeat unit could be determined. This topic is currently under investigation in our laboratory.

**Polystyrenes.** Several polystyrenes (PS) having various substituent groups at different positions on the hydrocarbon backbone or the benzene ring were studied. Part of the TOF-SIMS spectrum of polystyrene is shown in Figure 4 as a typical example. Polystyrene fragments cationized with $Ag^+$, $(nR + Ag)^+$ (R = 104 amu), produce the most intense peaks in the spectrum above $m/z$ 500; the spacing between them corresponds to the repeat unit of the polymer. The pattern of fragment ion peaks within the spacing of one repeat unit is consistent throughout the

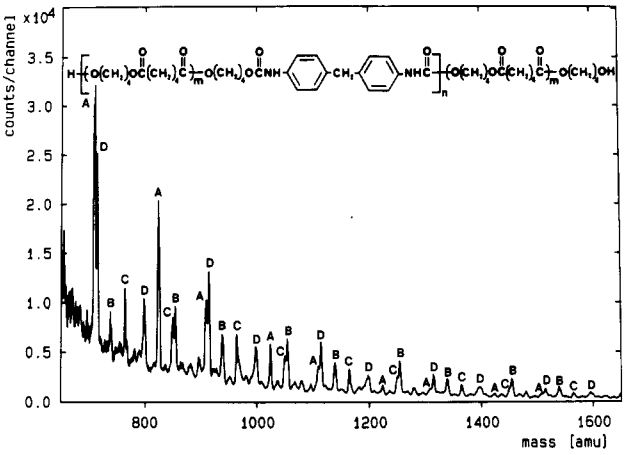


**Figure 3.** TOF-SIMS spectrum of a polyurethane in the range $m/z$ 650–1650. The peaks are identified by the letter of the series to which they correspond, i.e., (A) $(xA + M)^+$, (B) $(xB + M)^+$, (C) $(xC + M)^+$, and (D) $(xD + M)^+$, where M = Ag, Na and $x$ = 1, 2, 3, .... The structures of A, B, C, and D are given in the text.

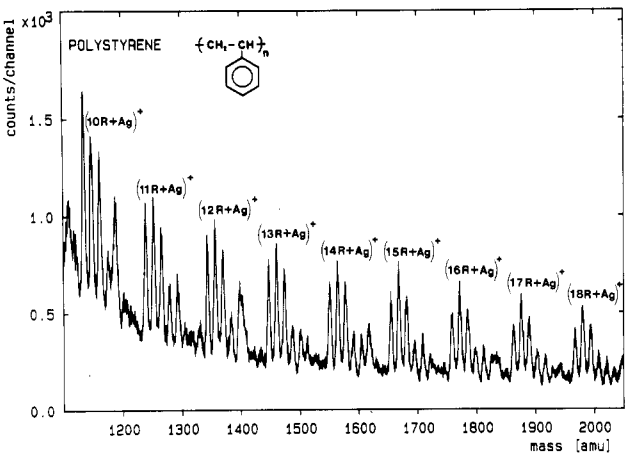


**Figure 4.** TOF-SIMS spectrum of polystyrene in the range $m/z$ 1100–2050. Peaks due to polystyrene fragments containing an integral number of repeat units and cationized with $Ag^+$ are identified. The fragmentation pattern within each repeat unit spacing is repeated throughout the spectrum.

spectrum and is characteristic of the repeat unit and its various substituent groups. For example, the peaks of the $(nR + Ag)^+$ series due to fragments containing 10 repeat units ($n$ = 10) for poly(*p-tert*-butylstyrene) (R = 160 amu) and poly(4-methoxystyrene) (R = 134 amu) appear at $m/z$ 1707 and 1447. The spacing between the $(nR + Ag)^+$ peaks for poly(*p-tert*-butylstyrene) is 160 amu and between the poly(4-methoxystyrene) is 134 amu. Therefore, from the peak position and the spacing between peaks the repeat units of polymers can be determined.

Poly($\alpha$-methylstyrene) (P($\alpha$-MS)) and poly(4-methylstyrene) (P(4-MS)) were studied to establish the effect of location of a substituent group on the TOF-SIMS spectrum. Specifically, it was sought to determine the effect of substituting a methyl group on a phenyl group and on the chain backbone. The repeat units of P($\alpha$-MS) and

**Table III**
**Fragments Observed for PUR in the Range $m/z$ 600–1700[a]**

A. $-[O(CH_2)_4OC(=O)(CH_2)_4C(=O)]_x- + M]^+$

| $x$ | M = Ag | M = Na | $x$ | M = Ag | M = Na |
|---|---|---|---|---|---|
| 3 | 707 (30309), 709 (31227)[b] | 623 (80367) | 6 | 1307 (1308) | 1223 (1630) |
| 4 | 907 (10170) | 823 (20341) | 7 | 1507 (795) | 1423 (832) |
| 5 | 1107 (3531) | 1023 (5886) | 8 | 1707 (451) | 1623 (559) |

B. $-[O(CH_2)_4OC(=O)NH-C_6H_4-CH_2-C_6H_4-NH-C(=O)[O(CH_2)_4OC(=O)(CH_2)_4C(=O)]_x-O(CH_2)_4OH + M]^+$

| | | | | | |
|---|---|---|---|---|---|
| 1 | 736 (9184), 738 (8266)[b] | 652 (17450) | 4 | 1336 (2378) | 1252 (4161) |
| 2 | 936 (6683) | 852 (9589) | 5 | 1536 (1505) | 1452 (2378) |
| 3 | 1136 (4075) | 1052 (6339) | 6 | 1736 (870) | 1652 (1397) |

C. $-[O(CH_2)_4OC(=O)(CH_2)_4C(=O)]_x-O(CH_2)_4OC(=O)NH-C_6H_4-CH_2-C_6H_4-NH-C(=O)- + M]^+$

| | | | | | |
|---|---|---|---|---|---|
| 1 | 647 (14287), 649 (14300)[b] | 563 (16073) | 4 | 1247 (2556) | 1163 (3357) |
| 2 | 847 (8719) | 763 (11021) | 5 | 1447 (1367) | 1363 (1783) |
| 3 | 1047 (4618) | 963 (6683) | 6 | 1647 (752) | 1563 (903) |

D. $-[O(CH_2)_4OC(=O)(CH_2)_4C(=O)]_xO(CH_2)_4OH + M]^+$

| | | | | | |
|---|---|---|---|---|---|
| 2 | 596 (21431), 598 (21500)[b] | 512 (48220) | 5 | 1196 (2626) | 1112 (5977) |
| 3 | 796 (10563), 798 (9643)[b] | 712 (24798) | 6 | 1396 (1486) | 1312 (2734) |
| 4 | 996 (5521) | 912 (13076) | 7 | 1596 (753) | 1512 (1333) |

[a] Peaks due to the silver doublet are seen only in the low-mass range because of spectrometer resolution. [b] Peak intensities are given in parentheses (counts/channel).

**Table IV**
**Relative Intensities of Cluster Peaks for P($\alpha$-MS) and P(4-MS) Appearing at $\pm n'\Delta m$ of the $(n\mathrm{R} + \mathrm{Ag})^+$ Series**

| polymer | $-4\Delta m$ | $-3\Delta m$ | $-2\Delta m$ | $-\Delta m$ | $(n\mathrm{R} + \mathrm{Ag})^+$ | $+\Delta m$ | $+2\Delta m$ | $+3\Delta m$ | $+4\Delta m$ |
|---|---|---|---|---|---|---|---|---|---|
| P($\alpha$-MS) | 34 | 91 | 87 | 80 | 100 | 19 | 16 | 13 | 13 |
| P(4-MS) | 50 | | | 100 | 91 | 67 | 51 | 48 | 43 |

P(4-MS) have equal masses, R = 118 amu; the most prominent peaks, due to $Ag^+$ cationized fragments $(n\mathrm{R} + \mathrm{Ag})^+$, for both P($\alpha$-MS) and P(4-MS) appear at exactly the same $m/z$ values. Therefore, it is not possible to distinguish between P($\alpha$-MS) and P(4-MS) by the positions and the spacings of these peaks. The $(n\mathrm{R} + \mathrm{Ag})^+$ peaks, however, are surrounded by a series of peaks of varying intensity spaced at $\pm n'\Delta m$, where $n' = 1, 2, 3$, and 4 and $\Delta m$ = 14–16 mass units. Data are shown for the two polymers in Table IV. The positions of the smaller peaks and their relative intensities are different in the two spectra, permitting one to distinguish readily between P(4-MS) and P($\alpha$-MS).

The differences in fragmentation are due to the different positions of the $-CH_3$ substituent group in the two polystyrenes. It was observed generally that substituent groups at different locations in the backbone or the benzene ring produce different fragmentation patterns for the polystyrenes. Bond cleavage seems to occur statistically, and the chemical stability of the fragments produced is reflected by the peak intensities. A more detailed discussion of fragmentation patterns for the polystyrenes studied will be published.[40]

**Oligomer Distributions.** MS is a useful technique for the determination of molecular weight distributions of low molecular weight polymers.[10,14,20,30] MS can provide information about the structure of the repeat unit and the number of repeat units for individual oligomers. In contrast, classical techniques used for determining molecular weights (e.g., gel permeation chromatography (GPC), vapor pressure osmometry, light scattering, nuclear magnetic resonance, etc.) measure average properties of an oligomer mixture and do not yield information on different types of oligomers present. Number- ($M_n$) and weight- ($M_w$) average molecular weights can be calculated readily from a mass spectrum by measuring the intensities of molecular or quasi-molecular ions for the various oligomers.

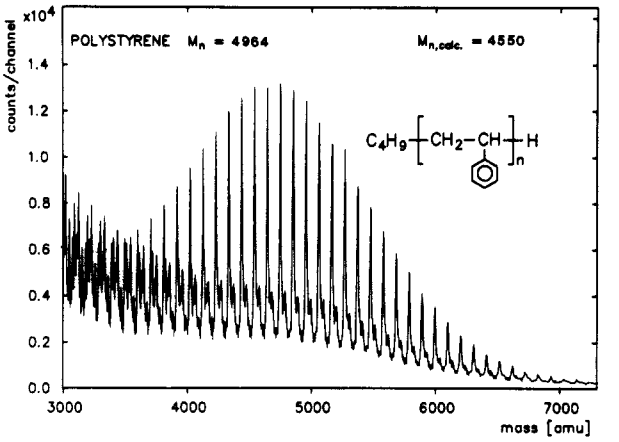


**Figure 5.** TOF-SIMS spectrum of polystyrene standard in the range $m/z$ 3000–7200, showing the distribution of polystyrene oligomers cationized with $Ag^+$. The number-average molecular weight determined by TOF-SIMS, $M_{n,calcd}$ = 4550, is within 8% of the value determined by GPC, $M_n$ = 4964.

Polymer molecular weight distributions obtained from TOF-SIMS spectra were evaluated by using polymer standards having known molecular weight distributions. A TOF-SIMS spectrum of a PS standard with $M_n$ = 4964 (determined by GPC) is shown in Figure 5. Below $m/z$ 3500, the most intense peaks are due to $Ag^+$ cationized polymer fragments corresponding to the series $(n\mathrm{R} + \mathrm{Ag})^+$. In the range $m/z$ 3500–7000, intact oligomers are detected

giving rise to the $(nR + C_4H_9 + H + Ag)^+$ series. These peaks are the most intense in this range, and their intensity distribution reflects the number-average molecular weight distribution of the PS standard. Loss of a terminal $-C_4H_9$ group results in the $(nR + Ag)^+$ series, having lower intensity than $(nR + C_4H_9 + H + Ag)^+$. The higher intensity of the $(nR + C_4H_9 + H + Ag)^+$ series indicates that even if some fragmentation occurs, the dominant process in the $m/z$ 3500–7000 range is desorption of intact polymer molecules cationized with $Ag^+$. The value $M_n = 4550$ was calculated from peak intensities without isotopic abundance corrections. The calculated value $M_n = 4550$ is within 8% of $M_n = 4964$ determined by GPC.

An important question to consider is whether fragmentation and ionization/desorption processes affect molecular weight distributions calculated from TOF-SIMS spectra. Fragmentation will interfere with ion quantitation if the fragmentation probabilities of individual oligomers vary with size. If it is assumed that polymer chains are randomly distributed on the Ag substrate and that the average distance between points of impact of argon ions on the sample target is constant, the probability for a long polymer chain to undergo fragmentation is higher than for a short one. In the lower part of the distribution range, fragments having a terminal $-C_4H_9$ group and whole polymer molecules with the $-C_4H_9$ terminal group intact will give rise to peaks that cannot be resolved. Consequently, the $(nR + C_4H_9 + H + Ag)^+$ series may appear to be more intense in the lower part of the distribution region (e.g., $m/z \sim 4000$) due to contributions from fragmentation. Such an effect will cause the distribution to be weighted toward lower molecular weight oligomers. Also, it has been established that the TOF-SIMS detection efficiency decreases with increasing mass.[41] An approximate correction was applied to the spectrum in Figure 5 to compensate for postacceleration and detection efficiencies; a corrected value of $M_n = 5600$ was obtained. Although approximate, the correction shifts the distribution in the right direction. The fragmentation and ionization/desorption processes, combined with the TOF-SIMS detection bias for small masses, shift the molecular weight distribution toward lower masses. This may explain the low $M_n$ value calculated from the TOF-SIMS spectrum. For the determination of more accurate molecular weight distributions, appropriate corrections for fragmentation, ionization/desorption, and detection efficiencies are necessary. A discussion of factors affecting molecular weight distributions of polymers obtained from TOF-SIMS spectra will be published in detail.[42]

## Conclusions

It has been shown that TOF-SIMS can be used effectively to characterize polymers up to mass 10 000. Fragmentation occurs consistently at specific bonds facilitating spectral interpretation. The spacing between consecutive peaks of the same series corresponds to the polymer repeat unit; therefore, polymers can be identified readily. Polymers having isobaric repeat units can be distinguished by differences in fragmentation patterns within each repeat unit. The oligomer distribution for a low molecular weight polymer was obtained; the $M_n$ value agreed well with that determined by GPC for the same polymer.

This report is intended to provide an overview of results from a new mass spectrometric technique that appears to have considerable value for practical polymer analysis. A detailed discussion of each topic presented above will be published separately.

**Acknowledgment.** This work was supported by the National Science Foundation under Grant CHE-8541141 and by the Deutsche Forschungsgemeinschaft. We are grateful to the Alexander von Humboldt Foundation for a senior fellowship for David M. Hercules, which stimulated this work. We are also grateful to Drs. C. Karakatsanis and J. Rieck of Mobay Chemical Corp. for providing the PUR samples.

**Registry No.** Polystyrene, 9003-53-6; (adipic acid) (butanediol) (MDI) (copolymer), 26375235.

## References and Notes

(1) Schulten, H.-R.; Lattimer, R. P. *Mass Spectrom. Rev.* **1984**, *3*, 231.
(2) Mol, G. T.; Gritter, R. J.; Adams, G. E. In *Applications of Polymer Spectroscopy*; Brame, E. G., Ed.; Academic: New York, 1978; pp 257–277.
(3) Evans, D. L.; Weaver, J. L.; Mukherji, A. K.; Beatty, C. L. *Anal. Chem.* **1978**, *50*, 857.
(4) Lüderwald, I.; Vogl, O. *Makromol. Chem.* **1979**, *180*, 2295.
(5) Sugimura, Y.; Nagaya, T.; Tsunge, S. *Macromolecules* **1981**, *14*, 520.
(6) Zeman, A. *Angew. Makromol. Chem.* **1973**, *31*, 1.
(7) Marshal G. L. *Eur. Polym. J.* **1983**, *19*, 439.
(8) Schulten, H.-R. *Int. J. Mass Spectrom. Ion Phys.* **1979**, *32*, 97.
(9) Uhr, B.; Lüderwald, I.; Müller, R.; Schulten, H.-R. *Angew. Makromol. Chem.* **1984**, *120*, 163.
(10) Matsuo, T.; Matsuda, H.; Katakuse, I. *Anal. Chem.* **1979**, *51*, 69.
(11) Lattimer, R. P.; Harmon, D. J.; Hansen, G. E. *Anal. Chem.* **1980**, *52*, 1808.
(12) Lattimer, R. P.; Schulten, H.-R. *Int. J. Mass Spectrom. Ion Phys.* **1983**, *52*, 105.
(13) Lattimer, R. P.; Hooser, E. R.; Diem, H. E.; Rhee, C. K. *Rubber Chem. Technol.* **1982**, *55*, 442.
(14) Lai, S.-T.; Chan, K. W.; Cook, K. D. *Macromolecules* **1980**, *13*, 953.
(15) Chait, B. T.; Shpungin, J.; Field, F. H. *Int. J. Mass Spectrom. Ion Processes* **1984**, *58*, 121.
(16) Gardella, J. A.; Hercules, D. M.; Heinen, H. J. *Spectrosc. Lett.* **1980**, *13*, 347.
(17) Gardella, J. A.; Hercules, D. M. *Fresenius' Z. Anal. Chem.* **1981**, *308*, 297.
(18) Graham, S. W.; Hercules, D. M. *Spectrosc. Lett.* **1982**, *15*, 1.
(19) Mattern, D. E.; Lin, F.-T.; Hercules, D. M. *Anal. Chem.* **1984**, *56*, 2762.
(20) Mattern, D. E.; Hercules, D. M. *Anal. Chem.* **1985**, *57*, 2041.
(21) Wilkins, C. L; Weil, D. A.; Yang, C. L.; Ijames, C. F. *Anal. Chem.* **1985**, *57*, 520.
(22) Brown, R. S.; Weil, D. A.; Wilkins, C. L. *Macromolecules* **1986**, *19*, 1255.
(23) Benninghoven, A.; Sichterman, W. K. *Anal. Chem.* **1978**, *50*, 1180.
(24) Gardella, J. A.; Hercules, D. M. *Anal. Chem.* **1980**, *52*, 226.
(25) Campana, J. E.; DeCorpo, J. J.; Colton, R. J. *Appl. Surf. Sci.* **1981**, *8*, 337.
(26) Briggs, D. *SIA, Surf. Interface Anal.* **1982**, *4*, 151.
(27) Briggs, D.; Hearn, M. J.; Ratner, B. D. *SIA, Surf. Interface Anal.* **1984**, *6*, 185.
(28) Gardella, J. A.; Hercules, D. M. *Anal. Chem.* **1981**, *53*, 1879.
(29) Gardella, J. A.; Novak, F. P.; Hercules, D. M. *Anal. Chem.* **1985**, *57*, 2041.
(30) Lattimer, R. P. *Int. J. Mass Spectrom. Ion Processes* **1983/84**, *55*, 221.
(31) Benninghoven, A. *J. Vac. Sci. Technol., A* **1985**, *3*, 451.
(32) Steffens, P.; Niehuis, E.; Friese, T.; Benninghoven, A. In *Ion Formation from Organic Solids*; Benninghoven, A., Ed.; Springer-Verlag: Berlin, 1983; Vol. 25, pp 111–117.
(33) Steffens, P.; Niehuis, E.; Friese, T.; Greifendorf, D.; Benninghoven, A. *J. Vac. Sci. Technol., A* **1985**, *3*, 1322.
(34) Bletsos, I. V.; Hercules, D. M.; Greifendorf, D.; Benninghoven, A. *Anal. Chem.* **1985**, *57*, 2384.
(35) Grade, H.; Cooks, R. G. *J. Am. Chem. Soc.* **1978**, *100*, 5615.
(36) Röllgen, F. W.; Borchers, F.; Giessmann, U.; Levsen, K. *Org. Mass. Spectrom.* **1977**, *12*, 541.
(37) Hunter, M. J.; Hyde, J. F.; Warrick, E. L.; Fletcher, H. J. *J. Am. Chem. Soc.* **1946**, *68*, 667.
(38) Kleinert, J. C.; Weschler, C. J. *Anal. Chem.* **1980**, *52*, 1245.
(39) Bletsos, I. V.; Hercules, D. M.; vanLeyen, D.; Benninghoven, A., to be published.
(40) Bletsos, I. V.; Hercules, D. M.; vanLeyen, D.; Benninghoven, A., to be published.
(41) Niehuis, E. Diploma Work, University of Münster, 1981.
(42) Bletsos, I. V.; Hercules, D. M.; van Leyen, D.; Benninghoven, A., to be published.